35th Annual International Conference of the IEEE EMBS
Osaka, Japan, 3 - 7 July, 2013

Linear Parameter Varying Identification of Ankle Joint Intrinsic Stiffness during Imposed Walking Movements*

Ehsan Sobhani Tehrani, Kian Jalaleddini, and Robert E. Kearney, *Fellow, IEEE*

Abstract— **This paper describes a *novel* model structure and identification method for the time-varying, intrinsic stiffness of human ankle joint during imposed walking (IW) movements. The model structure is based on the superposition of a large signal, linear, time-invariant (LTI) model and a small signal linear-parameter varying (LPV) model. The methodology is based on a two-step algorithm; the LTI model is first estimated using data from an *unperturbed* IW trial. Then, the LPV model is identified using data from a *perturbed* IW trial with the output predictions of the LTI model removed from the measured torque. Experimental results demonstrate that the method accurately tracks the *continuous-time* variation of normal ankle intrinsic stiffness when the joint position changes during the IW movement. Intrinsic stiffness gain decreases from full plantarflexion to near the mid-point of plantarflexion and then increases substantially as the ankle is dosriflexed.**

I. INTRODUCTION

Dynamic joint stiffness is defined as the dynamic relationship between a joint position and the torque acting about it. As such, it plays a critical role in voluntary movement since it defines the properties of the human actuator and internal load that the central nervous system (CNS) must control. Dynamic joint stiffness has two main components: (i) *Intrinsic* stiffness due to the passive visco-elastic and inertial properties of the limb, joint and connective tissue and the active properties of contracting muscle fibers; and (ii) *Reflex* stiffness originating from stretch reflex induced changes in muscle activation [1].

Joint stiffness varies with joint position and can be modulated by neural activation to counteract external perturbations and control voluntary movement. Numerous system identification studies have demonstrated this under quasi-stationary conditions. Mirbagheri *et al.* [2] estimated intrinsic and reflex components in normal subjects at operating points (OPs) that covered a wide range of joint positions and muscle contraction levels. They showed increase in both stiffness components as the ankle is dosriflexed and the activation level of the ankle muscles increased. Recently, Hyunglae *et al.* [3] used an OP-based impedance estimation method to show that stiffness increases with contraction level particularly in plantar/dorsiflexion (PF/DF) compared to inversion-eversion. Popescu *et al.* [4] estimated changes in elbow impedance during voluntary extension by applying brief random torque perturbations at various points of the movement. Moreover, numerous studies of the upper limb end-point stiffness [5], [6], [7] indicate that it varies systematically with the limb's kinematics and muscle activation. This is often demonstrated by visualizing changes in the shape (i.e., eccentricity and semi-major axis) of 2D or 3D ellipses representing *static*, time-invariant (TI) end-point stiffness matrix at various arm postural configurations. The major shortcomings of the above work are: (a) Often joint is perturbed at a series of dissociated OPs along the movement trajectory and TI system identification methods are used to obtain a *local* model at each OP. These OP studies are more relevant for postural tasks; it is not always trivial and analytically valid to simply interpolate the local models to represent the *global* time-varying (TV) behavior. (b) Some provide only *qualitative* or *implicit* descriptions of stiffness changes during movement without estimating the underlying functional relationships. This is required to discern the relative contributions of intrinsic biomechanical and neural factors quantitatively.

A number of studies are reported in the literature for TV identification of large and rapid changes in stiffness during different tasks. For example, Bennett *et al.* [8] used an ensemble-based method to identify TV mechanical properties of human elbow during cyclic movements. Kearney *et al.* [9] developed an identification method to estimate TV impulse response functions from an ensemble of input/output (I/O) data and used it to examine ankle stiffness changes during rapid, voluntary isometric contractions. Kirsch and Kearney [10] used the same method to demonstrate large transient changes in ankle stiffness during large passive imposed movements. More recently, Ludvig *et al.* [11] developed an ensemble-based TV extension of the TI non-parametric parallel-cascade algorithm [12] for the identification of both intrinsic and reflex stiffness. These ensemble-based methods have some shortcomings: (a) They cannot predict the biomechanical response of the joint to a novel trajectory of joint position since TV changes are identified as explicit functions of *time* without describing its functional relationship to the OP; and (b) They need trials with the same TV behavior which limits their utility mainly to repeatable movements.

This paper addresses the above shortcomings by developing a *novel*, linear-parameter varying (LPV) model structure and identification method. LPV models represent a class of nonlinear and/or TV systems with a model structure resembling that of a linear system but parameters that change as a function of a time-dependent signal called *scheduling variable* (SV) [13]. We believe that the LPV model structure

*This work has been supported by NSERC & CIHR.

E. Sobhani Tehrani and K. Jalaleddini are with the Department of Biomedical Engineering, McGill University, 3775 University, Montréal, Québec H3A 2B4, Canada. {ehsan.sobhani, seyed.jalaleddini}@ mail.mcgill.ca,

R. E. Kearney is with the Department of Biomedical Engineering, McGill University, 3775 University, Montréal, Québec H3A 2B4, Canada. robert.kearney@ mcgill.ca.

is well suited for representing TV systems since it provides strong predictive ability for novel system trajectories. Experimental results demonstrate that the method accurately tracks position-dependent changes in intrinsic ankle stiffness during imposed walking movements.

This paper is organized as follows: Section II formulates the time-varying stiffness identification problem using the LPV model structure. Section III describes the *novel* LPV methodology developed to solve it. Section IV presents the results of an experimental validation of the proposed technique. Section V provides some concluding remarks.

II. Problem Formulation

This section formulates the general problem of identifying TV joint biomechanics using an LPV model structure and then develops a specific solution for TV *intrinsic* stiffness. TV joint dynamics can be written as:

$$T(t) - T_v(t) = S(t, \theta(t)) \tag{1}$$

where T is total joint torque; T_v is voluntary torque; θ is joint position; t is time; and S is a nonlinear *dynamic* stiffness operator. If it is assumed that intrinsic and reflex torques add linearly, (1) can be rewritten as:

$$T(t) - T_v(t) = T_i(t) + T_r(t) = S_i(t, \theta(t)) + S_r(t, \dot{\theta}(t - \Delta_r)) \tag{2}$$

Where S_i and S_r are *dynamic* operators representing intrinsic and reflex stiffness; $\dot{\theta}(t) = d\theta/dt$ is the joint velocity; and Δ_r is the delay of the reflex pathway.

This paper will focus on TV *intrinsic* stiffness identification as the first step in a comprehensive solution. This representation shows TV stiffness as an explicit function of time. However, it seems likely that under many conditions changes in stiffness are not explicitly TV but result implicitly from dependence on variables such as position and activation level that vary with time:

$$T_i(t) = S_i\left(f_i\left(\overline{\theta}(t), \lambda(t)\right), \theta(t)\right) \tag{3}$$

where $\lambda(t)$ denotes the level of muscle activation; $\overline{\theta}(t)$ is the *trajectory of joint position OP* defined as the joint position excluding small signal perturbations used for identification; and f_i describes how intrinsic stiffness changes with $\overline{\theta}(t)$ and $\lambda(t)$.

Further assumptions are required regarding the model structure for f_i and S_i. In particular, it will be assumed that S_i can be represented by a model having inertial (*I*), viscous (*B*) and elastic (*K*) components and the parameters vary as static, nonlinear functions of $\overline{\theta}(t)$ and $\lambda(t)$. This makes intrinsic stiffness a function of the SV defined as:

$$\rho(t) \triangleq \left[\overline{\theta}(t) \quad \lambda(t)\right]^{\mathrm{T}} \tag{4}$$

We identify intrinsic ankle stiffness during an imposed walking (IW) movement at *rest* (i.e., subjects are asked *not* to voluntarily activate their muscles). Therefore, $\lambda(t) \cong 0, \forall t$ and the SV is:

$$\rho_{IW}(t) \triangleq \overline{\theta}(t) \tag{5}$$

And the model of intrinsic stiffness is represented by:

$$S_i(\rho_{IW}, \theta) = I(\rho_{IW}(t))\ddot{\theta}(t) + B(\rho_{IW}(t))\dot{\theta}(t) + K(\rho_{IW}(t))\theta(t) \tag{6}$$

where $\theta, \dot{\theta}, \ddot{\theta}$ are the *instantaneous* joint angular position, velocity, and acceleration, respectively. The *instantaneous position* $\theta(t)$ and *trajectory of joint position operating point* are related as follows:

$$\theta(t) = \overline{\theta}(t) + \Delta\theta(t) \tag{7}$$

where $\Delta\theta$ represents *random* small signal perturbations. $\overline{\theta}(t)$ can be calculated from measurements in two ways: (i) ensemble averaging of $\theta(t)$ in cyclic, repeatable movements and (ii) moving average of $\theta(t)$ in non-cyclic movements.

III. Identification Methodology

A. Model Structure

To identify the relationship between the *intrinsic stiffness* parameters and the SV during the IW trial, use (2) and (6) to write:

$$T \cong I(\rho_{IW})\ddot{\theta} + B(\rho_{IW})\dot{\theta} + K(\rho_{IW})\theta + T_r + n \tag{8}$$

where n is the output torque measurement noise. The dependence of (8) on t has been dropped for notational simplicity. Moreover, $T_v(t) \cong 0, \forall t$ in (2) because there is no voluntary activation at rest. Reflex torque in (8) is also regarded as a noise source which is correlated with input. However, it does *not* bias the estimates since it is negligible for large movements at rest.

Equation (8) is a lumped LPV *IBK* model representing both small signal and large signal intrinsic mechanics of the joint. We *hypothesize* that the large signal variations in intrinsic torque can be accurately described using an LTI model with constant coefficients. This hypothesis is supported by the utilization of IBK models for large movements like hopping and running. In contrast, the intrinsic stiffness response due to small signal perturbations along the trajectory of joint position operating point is modulated by the SV. Consequently, we use the model in (8) and (2) to obtain the following superposition of an LTI *IBK* and an LPV *IBK* model to represent the intrinsic stiffness:

$$T \cong \overline{I}\ddot{\overline{\theta}} + \overline{B}\dot{\overline{\theta}} + \overline{K}\overline{\theta} + I_{ss}\Delta\ddot{\theta} + B_{ss}(\rho_{IW})\Delta\dot{\theta} + K_{ss}(\rho_{IW})\Delta\theta + T_r + n \tag{9}$$

where $\dot{\bar{\theta}}$ is the rate of change in joint position operating point; $\Delta\dot{\theta}$ is the perturbation velocity; $\bar{I}, \bar{B}$ and $\bar{K}$ are the constant inertial, viscous and stiffness parameters of the LTI model; and B_{ss} and K_{ss} are the TV viscous and stiffness gains of the small signal LPV model, respectively. Moreover, since we assume *single* degree-of-freedom (1DOF) ankle motions in PF/DF direction, the *inertial* term I_{ss} in (9) is considered constant and independent of the SV.

The *nonlinear* dependence of B_{ss} and K_{ss} on the SV will be represented using Chebyshev polynomials as:

$$B_{ss}\left(\rho_{IW}\right) \cong \sum_{i=0}^{N_b} b_i g_i\left(\rho_{IW}\right); K_{ss}\left(\rho_{IW}\right) \cong \sum_{i=0}^{N_k} k_i g_i\left(\rho_{IW}\right) \tag{10}$$

where $g_i(\cdot)$ is the i^{th} basis function; b_i and k_i are the corresponding coefficients; and N_b and N_k are the orders of the expansions. The LPV parameters I_{ss}, $\left(b_i, i \in 0,1,...,N_b\right)$ and $\left(k_i, i \in 0,1,...,N_k\right)$, and the parameters $\bar{I}, \bar{B}$ and $\bar{K}$ in (9) are *unknown* and must be estimated from I/O data.

B. *Identification Algorithm*

The parameters of model (9) and (10) may be estimated using a 2-step algorithm that requires two trials with different conditions:

Step-1: Estimate the parameters of the LTI *IBK* model using I/O data of an *unperturbed* IW experiment, where *no* position perturbations are applied to the joint; thus $\Delta\theta = 0$ and $\theta = \bar{\theta}$ in (7). Moreover, with *no* perturbations, $T_r \cong 0$ and (9) can be written as a linear regression:

$$Y_1 = \Psi_1 \cdot \alpha_1 + N \tag{11}$$

where $Y_1 = \left\{T\left(t\right); t = 0,...,t_N\right\}$, $N = \left\{n\left(t\right); t = 0,...,t_N\right\}$, and t_N is the *duration* of a trial. The regressor matrix and the vector of coefficients are defined as follows:

$$\Psi_1 = \begin{bmatrix} \ddot{\theta}(0) & \dot{\theta}(0) & \theta(0) \\ \vdots & \ddots & \vdots \\ \ddot{\theta}(t_N) & \dot{\theta}(t_N) & \theta(t_N) \end{bmatrix} \tag{12}$$

$$\alpha_1 \triangleq \begin{bmatrix} \bar{I} & \bar{B} & \bar{K} \end{bmatrix}^{\mathrm{T}} \tag{13}$$

Estimate the parameters α_1 using least squares (LS).

Step-2: Use the LS estimates of (13) in (9) to estimate the coefficients of the LPV *IBK* model given in (10) using data from a *perturbed* IW trial, where $\Delta\theta \neq 0$. In this case, (9) is written as a linear regression:

$$Y_2 = \Psi_2 \cdot \alpha_2 + E \tag{14}$$

where $Y_2 = \left\{T\left(t\right) - \hat{\bar{I}}\ddot{\bar{\theta}}\left(t\right) - \hat{\bar{B}}\dot{\bar{\theta}}\left(t\right) - \hat{\bar{K}}\bar{\theta}\left(t\right); t = 0,...,t_N\right\}$ is the *large signal torque residual* defined as the difference between measured total ankle torque and the torque predicted by the LTI model; $E = \left\{T_r\left(t\right) + n\left(t\right); t = 0,...,t_N\right\}$; and $\hat{\bar{I}}, \hat{\bar{B}}$ and $\hat{\bar{K}}$ are the LS solution of (11). Here, the regressor matrix and the vector of coefficients in (14) are defined as:

$$\Psi_2 = \begin{bmatrix} G_b^{\mathrm{T}}\left(\rho_{IW}\left(0\right)\right) \otimes \Delta\dot{\theta}\left(0\right) & G_k^{\mathrm{T}}\left(\rho_{IW}\left(0\right)\right) \otimes \Delta\theta\left(0\right) \\ \vdots & \vdots \\ G_b^{\mathrm{T}}\left(\rho_{IW}\left(t_N\right)\right) \otimes \Delta\dot{\theta}\left(t_N\right) & G_k^{\mathrm{T}}\left(\rho_{IW}\left(t_N\right)\right) \otimes \Delta\theta\left(t_N\right) \end{bmatrix} \tag{15}$$

$$\alpha_2 \triangleq \begin{bmatrix} b_0 & \cdots & b_{N_b} & k_0 & \cdots & k_{N_k} \end{bmatrix}^{\mathrm{T}} \tag{16}$$

where $G_j\left(\rho_{IW}\right) = \left[g_0\left(\rho_{IW}\right), g_1\left(\rho_{IW}\right), \ldots, g_{N_j}\left(\rho_{IW}\right)\right]^{\mathrm{T}}$ with $j \in \left\{b, k\right\}$, and $\otimes$ is the Kronecker product.

IV. EXPERIMENTAL VALIDATION

The model and identification methodology were evaluated using experimental data acquired by imposing walking movements on a *normal* human ankle during rest.

A. *Method and Input Signal*

Four subjects, one female and three males, with no history of ankle pathologies were recruited. They gave informed consent to the experimental procedures which had been reviewed and approved by McGill University's *institutional review board*.

Subjects lay supine with the left foot attached by a custom built fiberglass boot [14] to the pedal of an electro-hydraulic actuator operating as a very stiff position servo. Two types of position inputs were used: (i) *Unperturbed IW (UIW)* where the ankle was moved through the *mean trajectory* of ankle PF/DF observed during normal gait [15], and (ii) *Perturbed IW (PIW)* where random PRBS perturbations were superimposed on the *mean trajectory* and applied to the ankle. The peak-to-peak amplitude of PRBS was set to 15% of that of the UIW trajectory. Subjects were instructed to remain relaxed throughout the experiment.

Joint angular position was measured using a potentiometer mounted on the actuator; the mid-position of the ankle was taken as zero, PF displacement taken as negative and DF as positive. Torque was measured with a very stiff torque transducer in series with the actuator and foot pedal. EMG was measured from *Tibialis Anterior* (TA) and three heads of *Triceps Surae* (TS) muscles (soleus, gastrocnemius medial and lateral heads) using Delsys surface EMG electrodes. EMG signals were pre-amplified by a gain of 1000 and high-pass filtered at 20 Hz to remove artifacts.

Signals were anti-alias filtered and then sampled at 1kHz. Both trials were lasted 70 seconds.

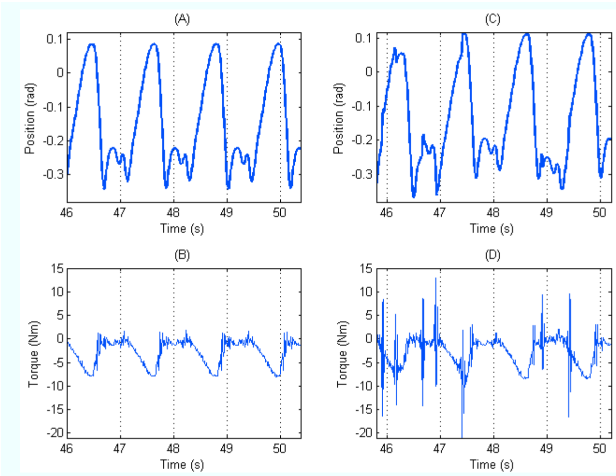

Figure 1. Four cycles of recorded joint (A) position and (B) torque in UIW; and (C) position and (D) torque in PIW trial at rest for a subject.

Fig. 1 shows the measured joint position and total torque for four cycles of the *UIW* (left column) and *PIW* trials (right column) for a typical subject. Each walking cycle lasted about 1.15 seconds; resulting in about 60 cycles in each trial. Short transient intrinsic torque responses are evident in the PIW trial associated with PRBS perturbations. It is also evident that the magnitude of these transients changes with the location of the perturbation along the walking trajectory.

The trajectory of position operating point $\overline{\theta}(t)$ used as the SV was estimated as the ensemble average of joint position for 60 cycles in the PIW record. The perturbation $\Delta\theta(t)$ was calculated as in (7) by subtracting the ensemble average from each PIW cycle.

EMGs from TA and Soleus muscles were monitored over the duration of all trials. Reflex responses *were not observed in any of the* UIW trials. In the PIW trials, reflex EMG responses were observed occasionally in the Soleus; however, since these were small and inconsistent in magnitude, they are not expected to *bias* intrinsic stiffness estimates.

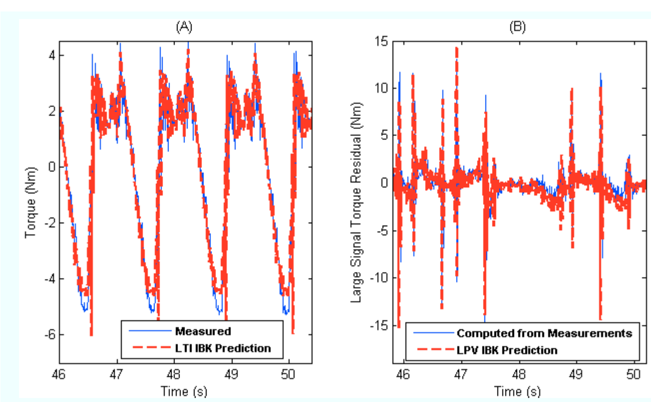

Figure 2. Prediction performance of the identified models: (A) LTI *IBK* model for measured torque of UIW and (B) LPV *IBK* model for *large signal torque residual* of PIW.

B. Results

Fig. 2 shows the torques predicted by identified models for a typical subject. Panel (A) shows the torque predicted by the LTI model superimposed on the measured torque for four cycles of the UIW trial. The percent of variance accounted for (%VAF) of the LTI model of each subject during UIW trials is given in Table I (column header: $\boldsymbol{\%VAF_{uiw}}$).

Panel (B) shows the torque predicted by the LPV model superimposed on the *large signal torque residual* for four cycles of the PIW trial. The %VAF of the LPV models of each subject during PIW trials is given in Table II (column header: $\boldsymbol{\%VAF_{ss}}$). The %VAF of the superposition of the LTI and LPV models of each subject in predicting the measured total torque of the PIW trials is also given in Table II (column header: $\boldsymbol{\%VAF_{piw}}$).

Table I shows the parameter estimates for the LTI model bracketed by their standard deviations (STD) for the four subjects. The STDs of the estimates were small compared to the estimated values indicating that the estimates were reliable. The LTI models of the four subjects consistently predicted near 96% of the torque variance in UIW trials.

TABLE I. ESTIMATED LTI IBK PARAMETERS AND THE %VAF OF THE MODELS FOR FOUR SUBJECTS USING DATA OF UIW TRIALS. NUMBERS IN BRACKETS ARE THE ESTIMATED STANDARD DEVIATIONS OF PARAMETERS.

Subject	$\overline{I}$ *(Nm.s²/rad)*	$\overline{B}$ *(Nm.s/rad)*	$\overline{K}$ *(Nm/rad)*	$\boldsymbol{\%VAF_{uiw}}$
S1	0.022 [1.6E-4]	0.51 [5.6E-3]	22.2 [0.05]	96.4
S2	0.016 [7.9E-5]	0.27 [2.4E-3]	9.3 [0.02]	96.5
S3	0.021 [1.8E-4]	0.50 [6E-3]	22.5 [0.05]	96.0
S4	0.021 [1.4E-4]	0.43 [4.6E-3]	19.4 [0.04]	96.8

Table II shows the estimated parameters of the elastic term of the LPV model and their STDs for the four subjects. The *coefficients of variation* for the identified parameters were below 0.16 for all subjects. We set the orders of the expansions in (10) to N_k =2 and N_b =0; using higher order expansions resulted in less than 0.05 increase in $\boldsymbol{\%VAF_{ss}}$ of the LPV models of all subjects. The superposition of the identified LTI and LPV models accurately predicted the joint torque of the PIW trials; $\boldsymbol{\%VAF_{piw}}$ was bigger than 92 for all subjects. Fig. 3 shows the identified curve of the intrinsic stiffness gain as a function of the position operating point for all subjects. The curves are normalized with the normalization factors (NF) given in the figure's legend. The figure reveals that for all subjects the intrinsic stiffness gain was low near mid-point of plantarflexion and increases towards full PF and DF positions. The rate of increase is significantly larger towards full DF position of the IW task.

Only the first term of the expansion of the LPV viscosity term was significant. This indicates that the viscosity was nearly *constant* over the position range used in IW trials. The estimated viscosity B_{ss} for the subjects S1 to S4 were 1.33 [0.014], 0.48 [0.007], 1.12 [0.015], and 0.96 [0.016] *Nm.s/rad* respectively. Both observations from the LPV *IBK* model are consistent with those made from small signal identification at multiple OPs [2, 16]. Finally, the estimated inertia of the LPV model I_{ss} for the subjects S1 to S4 were 0.022 [1.0E-4], 0.017 [5.2E-5], 0.020 [1.1E-4], and 0.022 [1.1E-4] $Nm.s^2/rad$ respectively. The numbers reported in brackets are the estimated STDs. The estimated inertias are consistent with those of the LTI models for all subjects.

TABLE II. ESTIMATED PARAMETERS OF THE STIFFNESS GAIN OF THE LPV IBK MODEL, THE %VAF OF THE LPV MODEL IN PREDICTING LARGE SIGNA TORQUE RESIDUAL, AND %VAF OF THE TOTAL TORQUE FOR FOUR SUBJECTS USING DATA OF PIW TRIALS. NUMBERS IN BRACKETS ARE THE ESTIMATED STANDARD DEVIATIONS OF PARAMETERS.

Subject	k_0	k_1	k_2	$\%VAF_{ss}$	$\%VAF_{piw}$
S1	-22.4 [0.5]	-15.3 [0.9]	-5.5 [0.87]	88.4	94.2
S2	-10.5 [0.2]	-6.1 [0.41]	-3.6 [0.41]	94.2	96.0
S3	-27.2 [0.5]	-18.9 [0.9]	-12.6 [0.9]	84.9	94.0
S4	-31.1 [0.6]	-22.3 [1.0]	-16.7 [1.0]	85.8	92.2

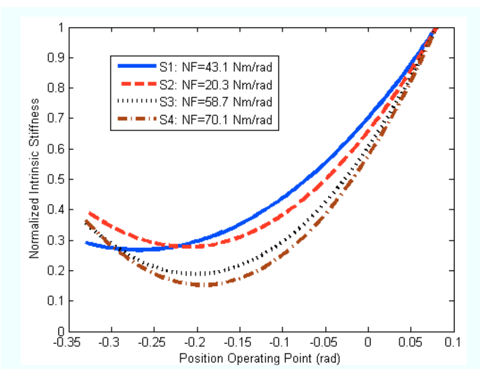

Figure 3. Identified intrinstic stiffness gain of the LPV *IBK* model as a function of joint position operating point in IW task at rest.

V. CONCLUSION

We presented a novel model structure and algorithm for identification of a *continuous-time* model of TV intrinsic stiffness while subjects perform an IW task at rest. The task involved large variations in ankle position as an operating point of the joint which is typically observed during many activities of daily living like normal gait. We estimated the variations of joint intrinsic stiffness parameters, particularly the elastic term, as a function of joint position operating point. The results demonstrated a significant increase in intrinsic stiffness gain, with a rate of a second-order polynomial, as the ankle was dosriflexed. These results are important because they provide models of joint intrinsic biomechanics and its variations during large-movement functional tasks with strong predictive ability.

The developed LPV model has three advantages: (a) It relates TV behavior to system variables that vary with time. This captures the nonlinear dynamics that generates the TV behavior. As a result, the estimated models can predict the response to novel trajectories. (b) It is a *global*, continuous-time model that is identified while the joint position operating point changes during movement without the need to identify and interpolate small signal, local models. (c) The LPV model is suitable for design of orthotic controllers since control theory is well developed for LPV models due to their structural similarities to linear systems.

The extension of the developed method to the parallel-cascade architecture for estimating joint stiffness variations when subjects maintain voluntary activation is a subject of future work. Furthermore, the developed methodology can be easily extended to the identification of 2D and 3D endpoint stiffness with all *IBK* terms varying as unknown functions of arm kinematics representing the SVs.

REFERENCES

[1] E. P. Widmaier, H. Raff, and T. K. Strang, *Vander's human physiology: the mechanisms of body function*, 11 ed. Boston: McGraw-Hill Higher Education, 2008.

[2] M. M. Mirbagheri, H. Barbeau, and R. E. Kearney, "Intrinsic and reflex contributions to human ankle stiffness: variation with activation level and position," *Experimental Brain Research,* vol. 135, pp. 423-436, Dec 2000.

[3] L. Hyunglae, W. Shuo, and N. Hogan, "Relationship between ankle stiffness structure and muscle activation," in *Engineering in Medicine and Biology Society (EMBC), 2012 Annual International Conference of the IEEE*, 2012, pp. 4879-4882.

[4] F. Popescu, J. M. Hidler, and W. Z. Rymer, "Elbow impedance during goal-directed movements," *Exp Brain Res,* vol. 152, pp. 17-28, Sep 2003.

[5] E. J. Perreault, R. F. Kirsch, and P. E. Crago, "Voluntary control of static endpoint stiffness during force regulation tasks," *J Neurophysiol,* vol. 87, pp. 2808-16, Jun 2002.

[6] N. Hogan, "The mechanics of multi-joint posture and movement control," *Biol Cybern,* vol. 52, pp. 315-31, 1985.

[7] X. Hu, W. M. Murray, and E. J. Perreault, "Muscle short-range stiffness can be used to estimate the endpoint stiffness of the human arm," *J Neurophysiol,* vol. 105, pp. 1633-41, Apr 2011.

[8] D. J. Bennett, J. M. Hollerbach, Y. Xu, and I. W. Hunter, "Time-Varying Stiffness of Human Elbow Joint during Cyclic Voluntary Movement," *Experimental Brain Research,* vol. 88, pp. 433-442, Feb 1992.

[9] J. B. Macneil, R. E. Kearney, and I. W. Hunter, "Identification of Time-Varying Biological-Systems from Ensemble Data," *Ieee Transactions on Biomedical Engineering,* vol. 39, pp. 1213-1225, Dec 1992.

[10] R. F. Kirsch and R. E. Kearney, "Identification of time varying stiffness dynamics of the human ankle joint during an imposed movement," *Experimental Brain Research,* vol. 114, pp. 71-85, Mar 1997.

[11] D. Ludvig, T. S. Visser, H. Giesbrecht, and R. E. Kearney, "Identification of Time-Varying Intrinsic and Reflex Joint Stiffness," *Ieee Transactions on Biomedical Engineering,* vol. 58, pp. 1715-1723, Jun 2011.

[12] R. E. Kearney, R. B. Stein, and L. Parameswaran, "Identification of intrinsic and reflex contributions to human ankle stiffness dynamics," *Ieee Transactions on Biomedical Engineering,* vol. 44, pp. 493-504, Jun 1997.

[13] P. dos Santos, T. Perdicoulis, and C. Novara, *Linear Parameter-Varying System Identification: New Developments and Trends*: World Scientific, 2012.

[14] R. L. Morier, P. L. Weiss, and R. E. Kearney, "Low Inertia, Rigid Limb Fixation Using Glass-Fiber Casting Bandage," *Medical & Biological Engineering & Computing,* vol. 28, pp. 96-99, Jan 1990.

[15] R. E. Kearney, M. Lortie, and R. B. Stein, "Modulation of stretch reflexes during imposed walking movements of the human ankle," *J Neurophysiol,* vol. 81, pp. 2893-902, Jun 1999.

[16] P. L. Weiss, R. E. Kearney, and I. W. Hunter, "Position dependence of ankle joint dynamics—I. Passive mechanics," *Journal of Biomechanics,* vol. 19, pp. 727-735, 1986.